Charge transfer in time-dependent density-functional theory via spin-symmetry breaking

Johanna I. Fuks,[1] Angel Rubio,[1,2] and Neepa T. Maitra[3]

[1]*Nano-Bio Spectroscopy Group and ETSF Scientific Development Centre, Departamento de Física de Materiales,*
Universidad del País Vasco, CFM CSIC-UPV/EHU-MPC, and DIPC, Avenida Tolosa 72, E-20018 San Sebastián, Spain
[2]*Fritz-Haber-Institut der Max-Planck-Gesellschaft, Faradayweg 4–6, D-14195 Berlin, Germany*
[3]*Department of Physics and Astronomy, Hunter College and City University of New York, 695 Park Avenue, New York, New York 10065, USA*

Long-range charge-transfer excitations pose a major challenge for time-dependent density-functional approximations. We show that spin-symmetry breaking offers a simple solution for molecules composed of open-shell fragments, yielding accurate excitations at large separations when the acceptor effectively contains one active electron. Unrestricted exact-exchange and self-interaction-corrected functionals are performed on one-dimensional models and on the real LiH molecule within the pseudopotential approximation to demonstrate our results.

Although time-dependent density-functional theory (TDDFT) has had resounding success in predicting accurate excitation spectra in a wide variety of systems [1,2], difficulties still plague its application to certain areas. The problem of charge-transfer (CT) excitations has drawn especially significant attention in recent years [3–9], due to its relevance for biomolecules, molecular conductance, and solar cell design; these are systems for which TDDFT would be particularly attractive due to its favorable system-size scaling. However, it has been challenging to find a satisfactory universal solution to the CT problem: *Ab initio* approaches based on modeling the exact kernel appear impractical, while practical approaches tend to involve empirical parameters. Here we present an approach to calculate CT excitations in TDDFT for certain cases, based on spin-symmetry breaking. We show that accurate excitations are obtained when the acceptor is an effectively one-electron system—for instance, an element in group 1 of the periodic table treated in the pseudopotential approximation—and justify why this is so. For large separations, the leading-order behavior is captured solely from Kohn-Sham (KS) orbital energy differences. Results are given for model systems and for the LiH molecule, and suggest a type of Koopmans' concept for one-electron systems.

The usual approximations in TDDFT notoriously underestimate CT excitations between fragments at large separations R. To leading order in $1/R$, the exact answer for the lowest CT frequency is

$$\omega_{CT}^{exact} \rightarrow I^D - A^A - 1/R, \qquad (1)$$

where I^D is the ionization energy of the donor, A^A is the electron affinity of the acceptor, and $-1/R$ is the first electrostatic correction between the now-charged species. (Atomic units are used throughout.) It is well understood why TDDFT severely underestimates CT [3–6]: In TDDFT, the first step is to compute the KS orbital energy differences between occupied (i) and unoccupied (a) orbitals, $\omega = \epsilon_a - \epsilon_i$. In a second step, these frequencies are corrected to the true excitations via the Hartree-exchange-correlation kernel, $f_{HXC}[n_0](\mathbf{r},\mathbf{r}',\omega)$, which shifts and mixes the KS excitations within a matrix formulation. The kernel is a functional of the ground-state density $n_0(\mathbf{r})$, with matrix elements $\int d^3r\, d^3r'\, \phi_i(\mathbf{r})\phi_a(\mathbf{r}) f_{HXC}(\mathbf{r},\mathbf{r}',\omega)\phi_{i'}(\mathbf{r}')\phi_{a'}(\mathbf{r}')$. For CT excita-

tions, the vanishing spatial overlap at large separations between occupied donor and unoccupied acceptor orbitals for different nuclei means that the TDDFT predictions for CT excitations reduce to the KS orbital energy difference, $\epsilon_a - \epsilon_i$, when using the usual semilocal functional approximations for f_{HXC}. With approximate ground-state functionals, the highest occupied molecular orbital (HOMO) energy, ϵ_H, underestimates the true ionization energy, while the lowest unoccupied molecular orbital (LUMO), ϵ_L, lacks relaxation contributions to the electron affinity. The last few years have seen many methods to correct the underestimation of CT excitations, e.g. Refs. [7–9]; most modify the ground-state functional to correct the approximate KS HOMO's underestimation of I, and mix in some degree of Hartree-Fock approximation, and most, but not all [8,9] determine this mixing via at least one empirical parameter. Fundamentally, staying within pure DFT, both the relaxation contributions to A and the $-1/R$ tail in Eq. (1) come from f_{HXC}, which must exponentially diverge with fragment separation [5,6]. Worse, in the case of open-shell fragments, *not* covered by most of the recent fixes, the exact f_{xc} in addition is strongly frequency dependent [6].

The major reason for the awkward kernel structure in the case of open-shell fragments lies in the KS ground-state description: The HOMO (and LUMO) are delocalized over the whole molecule, quite distinct from the Heitler-London-like nature of the true wave function. In the case of either the exact or the semilocal approximation, their orbital energy difference tends to zero as the molecule is pulled apart, so f_{HXC} must be responsible for the entire CT energy [6]. It has long been recognized that this static correlation error [10] is the root of the problem of poor *ground-state* energies, studied extensively in such molecules as H_2 [11], and that a simple way out is to allow the system to break spin symmetry. An unrestricted calculation with an approximate functional run on a diatomic molecule leads, at a critical internuclear separation, to the spin-polarized solution obtaining the lowest ground-state energy. Albeit having incorrect spin symmetry, accurate ground-state energies are achieved essentially because the KS description is rendered to have one electron on each atom.

Although less discussed, the same physics applies for heteroatomic molecules composed of open-shell fragments

[12], which suggests that symmetry breaking could be a means to obtain its CT excitations. If the exact functional were used, the lowest energy state remains correctly spin unpolarized at any R, but at the cost of stark step and peak features in the bonding region and a strong frequency-dependent structure in f_{HXC}, both of which difficult for approximations to capture. If, instead, correct spin symmetry is imposed on any existing approximate density functional, the ground state displays unphysical fractional charges at large R, delocalized HOMO and LUMO orbitals, and again poor CT energies [6,12].

The following examples show that remarkably accurate CT excitations can indeed be obtained from TDDFT via spin-symmetry breaking when the acceptor contains effectively one active electron; for large enough separations, these are contained in simply the bare KS excitations. We first present one-dimensional models that enable us to compare with highly accurate numerically exact solutions (computed using a Runge-Kutta differential equation solver implemented in the OCTOPUS code [13]), and then to analyze and understand in detail why the CT in symmetry-broken TDDFT is accurate via the underlying potentials. For the DFT calculations, we study the exact exchange (EXX) and the local-spin-density approximation (LSD) [14] with a self-interaction correction (SIC). We shall see that their correct long-range behavior yields the correct R dependence at large separations. We stress that this long-rangedness must be combined with symmetry breaking in order to get accurate CT excitations: Restricted calculations using these functionals fail [15]. The functionals are implemented in OCTOPUS within the Krieger-Li-Iafrate (KLI) approximation to the optimized effective potential (OEP) [16]. After studying the models, we then turn to the real LiH molecule.

I. WHY SYMMETRY BREAKING WORKS?

In our first model, the nuclear potentials are represented by short-range wells at separation R:

$$v_{\text{ext}}(x) = -U^L/\cosh^2(x) - U^R/\cosh^2(x - R), \quad (2)$$

where the strength $U^L = 5.5$ a.u. and $U^R = 6$ a.u. We place two electrons interacting soft-Coulombically via

$$v_{\text{ee}}(x,x') = 1/\sqrt{1 + (x - x')^2} \quad (3)$$

into this heteroatomic molecule. The unrestricted KS calculation yields a spin-unpolarized solution until a separation of $R \approx 2.3$ a.u. (coinciding with an avoided crossing in the potential energy surfaces [12]), where it begins to break symmetry: The eigenvalues for the up and down spins in the ground state begin to separate, and they slowly approach those of the isolated wells as the molecule is pulled farther apart and each electron settles in a different well. In contrast to Ref. [17], localization of orbitals is in fact achieved within KLI: For two electrons KLI is equivalent to full OEP, but even for systems of more than two electrons (not shown here) KLI yielded spin-polarized localized orbitals.

Figure 1 plots the lowest orbital excitation energies of the model in Eqs. (2) and (3). The KS energy differences, especially those of EXX, capture the exact CT excitations throughout with remarkable accuracy.
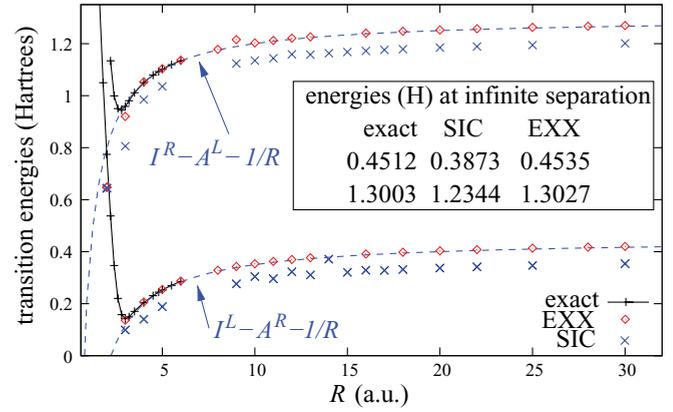

FIG. 1. (Color online) Charge-transfer excitation energies for the model in Eqs. (2) and (3) using unrestricted SIC and EXX. Exact convergence onto the asymptotic Eq. (1) (dashed gray lines; blue online) occurs soon after the symmetry-breaking point.

Why this is so can be seen by studying the underlying KS potentials. Consider first the limit $R \to \infty$, where symmetry breaking has placed, say, the spin-up (-down) electron in the left (right) well in the ground state. The left well is the donor for the following discussion. Figure 2 plots the KS potential for the ↑ spin,

$$v_{\text{s},\uparrow}[n_\uparrow, n_\downarrow] = v_{\text{ext}}^A + v_{\text{ext}}^D + v_{\text{H}}[n_\uparrow] + v_{\text{H}}[n_\downarrow] + v_{\text{xc},\uparrow}[n_\uparrow, n_\downarrow], \quad (4)$$

and its components at a separation of $R = 50$ a.u. In Eq. (4), $v_{\text{ext}}^{A(D)}$ refers to the atomic acceptor (donor) potential [i.e., the right (left) well], and $v_{\text{H}}[n](\mathbf{r}) = \int d^3r' n(\mathbf{r}')/|\mathbf{r} - \mathbf{r}'|$ is the Hartree potential generated by density $n(\mathbf{r})$. As $R \to \infty$, in the vicinity of the donor $v_{\text{c},\uparrow} = 0$ and $v_{\text{x},\uparrow} = -v_{\text{H}}[n_\uparrow]$, so $v_{\text{s},\uparrow} = v_{\text{ext}}^D$: The system is essentially a one-electron system in this limit, and local excitations of the ↑ electron are, correctly, just excited states of the donor. In the vicinity of the acceptor, where only a ↓ electron lives, $v_{\text{x},\uparrow} \to 0$ in the limit $R \to \infty$, and

$$v_{\text{s},\uparrow}^\infty(\mathbf{r} \sim \text{acceptor}) = v_{\text{ext}}^A + v_{\text{H}}[n_\downarrow] + v_{\text{c},\uparrow}[n_\uparrow, n_\downarrow]. \quad (5)$$
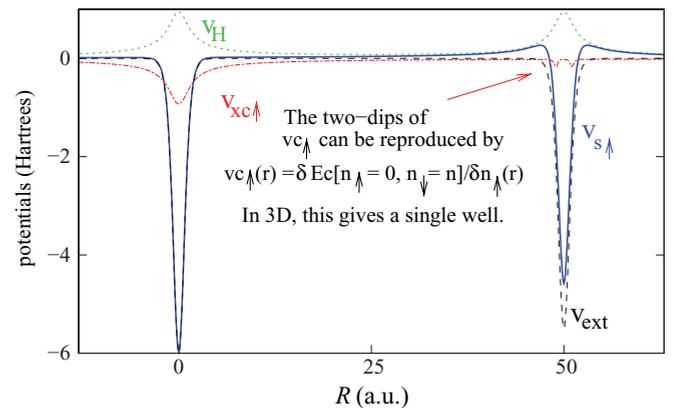

FIG. 2. (Color online) The KS potential $v_{\text{s},\uparrow}$ (solid line, blue online) and its components, as indicated. The dashed line (black online) is v_{ext}, the dotted line (green online) is v_H, and the dash-dotted line (red online) is $v_{\text{xc},\uparrow}$.

The Hartree potential generated by the $\downarrow$ electron and a small correlation contribution (the two dips in the red curve in the online version of Fig. 2) result in a net upward shift of v_{ext}: The unoccupied $\uparrow$-electron states living in the right-hand well are shifted upward in energy compared with those of the $\downarrow$ electron (i.e., those of v_{ext}). An approximate *affinity* level is thereby induced in the right-hand well. So the bare KS orbital energy differences yield accurate CT excitations: First, the HOMO for the $\uparrow$ electron is the lowest orbital in the left-hand well, for which $\epsilon_{\text{H}} = -I^D$, the exact ionization potential, due to Koopmans' theorem [18], since both EXX and SIC are exact for one electron. Second, and more significantly, the LUMO approximates the affinity level of the right-hand well, $\epsilon_{\text{L}} \approx -A^A$, sensing the presence of the $\downarrow$ electron, because Hartree-correlation relaxation contributions to the affinity are already incorporated at the bare KS level. We call this eigenstate of Eq. (5), and the corresponding state of $v_{\text{s},\downarrow}$, for which an entirely analogous analysis holds, the "induced affinity" levels of the right and left atoms respectively. In the limit of infinite separation, they converge onto the lowest state for the unoccupied spin of the isolated one-electron atom. A key point is that $v_{\text{s},\uparrow}$ and $v_{\text{s},\downarrow}$ are different: in any restricted calculation where these are the same, unoccupied levels are *excitations* (of the same N-electron system), not *affinities*.

How well does the induced affinity level approximate the true affinity level generally? Density-functional theory tells us that the exact affinity of an N-electron atom is $A(N) = E(N) - E(N+1) = -\epsilon_{\text{H}}(N+1)$, where the middle expression is computed from total energy differences, while the third expression is computed from the highest occupied KS eigenvalue of the relaxed $(N+1)$-electron system (see, e.g., [19]). Let us then consider the KS potential of a two-electron atom. Because the density is localized, an unrestricted calculation yields a spin-unpolarized result. If we denote the two-electron ground-state density as $n_2(\mathbf{r})$, we have

$$v[n_2] = v_{\text{ext}} + v_{\text{H}}[n_2/2] + v_{\text{c}}[n_2], \qquad (6)$$

where v_{ext} is the nuclear potential, and we have noted that, for exact exchange, $v_{\text{x}}[n_2] = -v_{\text{H}}[n_2]/2 = -v_{\text{H}}[n_2/2]$. First, by neglecting correlation, Eq. (6) is very close to Eq. (5) *if* $n_2 \approx 2n_\downarrow$—that is, if, when a second electron is added to a well in which there is already one electron, there is little density relaxation. This is the case in the model example above, since the dominant part of the energy of the electrons is from the external potential. In such a case, Eqs. (5) and (6) then imply that the induced affinity level approximates the true affinity well. It will be a lower bound [i.e., $|\epsilon_{L,\uparrow}| \leqslant |\epsilon_H(N=2)|$], because electron repulsion leads to $v_{\text{H}}[n_2/2]$ being a little weaker than $v_{\text{H}}[n_\downarrow]$. This was borne out in all of the EXX results of different models we considered. Correlation tends to raise the induced affinity, sometimes bringing it higher than the true affinity: Certainly using LSD-SIC, $v_{c,\uparrow}[n_\uparrow = 0, n_\downarrow = n]$ forms a deeper negative well than $v_c[n_2]$. Shortly we will discuss examples in which the density relaxation is important, so that n_2 is not very close to $2n_\downarrow$, and there the affinity level is not such a good approximation to the true affinity; consequently the CT excitations are not as accurate (but, as we will argue, the approach can still be useful).

The arguments above hold only for one-electron acceptors: If the acceptor already has an electron of the transferring spin in it, then excitations of that spin are the usual constant-number excitations of TDDFT, not approximate affinity levels. The donor, however, may contain any number of electrons: Similar models that have, for example, three electrons in one well and one in another have again showed excellent CT excitations from the former to the latter, under spin-symmetry breaking.

We now extend the discussion following Eq. (4) to the case of an N-electron donor and a one-electron acceptor, at finite but large separation. For ease of notation, assume again that the acceptor carries a $\downarrow$ electron in the molecular ground state. First consider Eq. (4) near the N-electron donor. For external (nuclear) potentials that exhibit Coulomb decay, the (N-electron) equivalent is $v_{\text{s},\uparrow} \sim v_s^D + O(1/R^3)$, where v_s^D is the KS potential of the donor atom. At the acceptor, $v_{\text{s},\uparrow} \sim v_{\text{s},\uparrow}^\infty - 1/R + O(1/R^3)$ (noting that v_{ext} cancels $v_{\text{H}}[n_\uparrow] \approx N^D/R$, while $v_{\text{x},\uparrow} \sim -1/R$). So, to leading order in R, for the $\uparrow$ electron, $\epsilon_{\text{H}} = \epsilon_{\text{H}}^D$ and $\epsilon_{\text{L}} = \epsilon_{\text{L}}^\infty - 1/R$, where $\epsilon_{\text{L}}^\infty$ is the induced affinity level of the acceptor in the infinite-separation limit. Therefore,

$$\omega_{\text{S}} = \epsilon_{\text{L}} - \epsilon_{\text{H}} = \epsilon_{\text{L}}^\infty - \epsilon_{\text{H}}^D - 1/R, \qquad (7)$$

as in Eq. (1), with $I^D \approx -\epsilon_{\text{H}}^D$ and A^A approximated by the induced affinity level. [For short-range potentials, as in Eq. (2), the arguments lead instead to $\epsilon_{\text{H}} = \epsilon_{\text{H}}^D + 1/R$ and $\epsilon_{\text{L}} = \epsilon_{\text{L}}^\infty$]. Therefore, a long-range exchange correlation as in EXX or SIC, once its symmetry is broken, yields good CT excitations, from just its bare KS orbital energies, as a function of R, for large R. Note the importance of correct asymptotics of the functional used for correct R dependence, as well as for accurate ionization potentials and induced affinities.

For an accurate CT asymptote, the density relaxation upon the addition of an electron must be small. But even when density relaxation effects are significant, symmetry breaking can still be useful, as we now explain.

In a practical sense, the infinite-separation limit itself is not so much a problem for TDDFT, because total ground-state energy differences computed from DFT [20] can often yield reliable values for I and A in Eq. (1). Rather, intermediate to large distances are the challenge, where CT energies deviate from the asymptotic formula in Eq. (1). Our symmetry-breaking approach can capture these deviations, going beyond Eq. (1). The procedure is to compute the (symmetry-broken) KS HOMO and LUMO energy difference, but when density relaxation is large, to shift it by

$$I^D - A^A - \left(\epsilon_{\text{L}}^{\infty,A} - \epsilon_{\text{H}}^D\right), \qquad (8)$$

where I and A are computed from total ground-state DFT energy differences. In this way, asymptotically, the curves approach Eq. (1) accurately, but for intermediate to large distances, they contain correct physical deviations from Eq. (1) due to polarization. To illustrate this, we now consider soft-Coulomb nuclear wells,

$$V_{\text{ext}} = -1/\sqrt{x^2 + a_L} - 1/\sqrt{(x-R)^2 + a_R}, \qquad (9)$$

and Fig. 3 takes $a_R = 0.7$ a.u. and $a_L = 1.2$ a.u.. The more diffuse densities of these wells make them more polarizable, so deviations from Eq. (1) are more evident, as shown in Fig. 3:
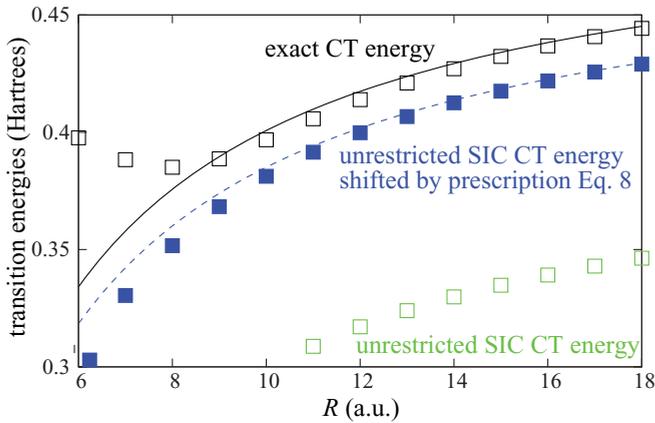
FIG. 3. (Color online) CT from the left to the right well of the model from Eq. (3) and Eq. (9). The exact calculation yields $I^D = 0.6206$ hartrees and $A^A = 0.1199$ hartrees. The unrestricted SIC calculation yields $I^D = \epsilon_H^D = 0.6206$ hartrees, $A^A = 0.1355$ hartrees, and $\epsilon_L^{\infty,A} = 0.2183$ hartrees.

At intermediate separations, the (exact) CT energies fall shy of the asymptotic Eq. (1), shown as the upper, solid black curve, due to the local polarization of the CT state toward the positive charge at the other nucleus. After applying the shift of Eq. (8), the unrestricted SIC results approach the exact results well and capture this attractive shift; this holds also for CT in the other direction (not shown in the figure). [The lower curve (blue online) is the asymptote for the unrestricted SIC prediction, but also shifted according to Eq. (8)].

So far, we have discussed CT excitations obtained from bare KS excitations alone and argued why these work so well, as demonstrated by the model examples. The second step of TDDFT is to apply f_{HXC} to correct the KS excitations toward the exact ones; there are both "diagonal" terms that shift each KS excitation, as well as "off-diagonal" ones that mix them. For the systems so far discussed, we expect that both these effects are small, because (i) the diagonal term involves overlap of the occupied and unoccupied orbitals in the excitation, which vanish exponentially at large distances, and (ii) there is little mixing with other excitations in the system. Mixing and shifting of KS excitations will be important at small and intermediate distances, leading to further deviations from the asymptotic Eq. (1), especially for real molecules, given their higher density of states.

A. The real LiH molecule

We turn now to a real molecule, LiH: Using a pseudopotential for the Li atom renders it an effectively one-electron atom, and our method captures CT in both directions. In Fig. 4, we plot the lowest potential energy surfaces of the LiH molecule, computed with unrestricted SIC, with the Troullier Martins pseudopotential coded in OCTOPUS [13], compared to the highly accurate configuration-interaction (CI) calculations of [21]. The induced affinity level of Hydrogen (H) is 0.0726 hartrees, while that computed from ground-state DFT energy differences is 0.0264 hartrees, closer to the experimental value (0.0277 hartrees), so we have applied the shift of Eq. (8) for $R \geqslant 12$ a.u. As accurate energies are unavailable for
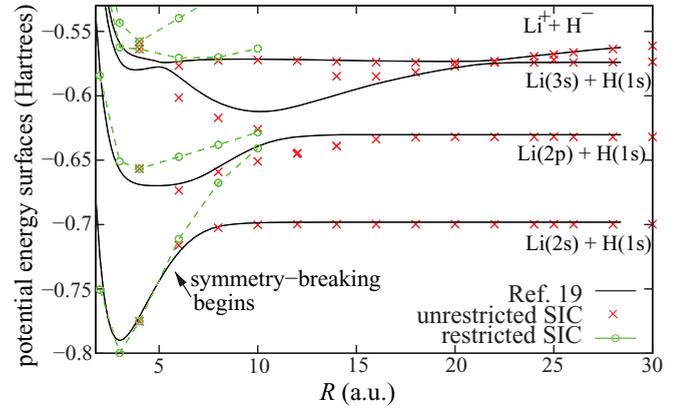

FIG. 4. (Color online) Potential energy surfaces of the LiH molecule. Even the (shifted) bare KS energy differences of unrestricted SIC are close to the configuration-interaction differences of [21].

CT from H to Li, we do not show this curve here. The excellent agreement of the unrestricted approach with CI, even at the bare KS level (i.e., no f_{HXC} applied), can be contrasted with spin-restricted SIC calculations, whose collapse at smaller R is due to the near-degeneracy of the HOMO and LUMO mentioned earlier; the latter leads to convergence difficulties for larger separations. The symmetry-broken SIC predicts the separation at which there is a crossing between the ionic curve and the Li(3s) curve very accurately ($R \approx 22$ a.u.), although it appears more as a direct crossing rather than an avoided one, at least in the bare KS orbital energy difference.

II. CONCLUSIONS

In summary, we have shown that symmetry breaking is a simple nonempirical way to obtain CT excitations from KS orbital energies alone, for acceptors that contain effectively one electron, and explained why. Strikingly good results were obtained for model systems as well as for the real molecule LiH, and further studies are under way. Applying the TDDFT kernel should improve the accuracy at intermediate distances, capturing mixing of CT and local excitations, while these f_{HXC} corrections will vanish asymptotically.

Conceptually, the observation that for one-electron systems, the levels of the unoccupied spin approximate affinity levels can be interpreted in an extended Koopmans sense. Koopmans' theorem in DFT states that $I = -\epsilon_H$ exactly, while a generalized Koopmans' theorem applies to Hartree-Fock where $I \approx -\epsilon_H^{HF}$ and $A \approx -\epsilon_L^{HF}$, leading to the use of hybrid functionals for CT, mentioned earlier [7,8]. Although the LUMO in exact DFT represents an excitation of the N-electron system, rather than of the $(N + 1)$-electron system, our results show that when $N = 1$ in spin DFT, the levels of the unoccupied spin can be interpreted in a generalized Koopmans sense because they approximate affinity levels.

[1] *Time-Dependent Density Functional Theory*, edited by M. A. L. Marques, C. A. Ullrich, F. Nogueira, A. Rubio, K. Burke, and E. K. U. Gross (Springer, Berlin, 2006).

[2] E. Runge and E. K. U. Gross, Phys. Rev. Lett. **52**, 997 (1984).

[3] A. Dreuw, J. Weisman, and M. Head-Gordon, J. Chem. Phys. **119**, 2943 (2003).

[4] D. Tozer, J. Chem. Phys. **119**, 12697 (2003).

[5] O. Gritsenko and E. J. Baerends, J. Chem. Phys. **121**, 655 (2004); J. Neugebauer, O. Gritsenko, and E. J. Baerends, *ibid.* **124**, 214102 (2006).

[6] N. T. Maitra, J. Chem. Phys. **122**, 234104 (2005); N. T. Maitra and D. G. Tempel, *ibid.* **125**, 184111 (2006).

[7] Y. Tawada *et al.*, J. Chem. Phys. **120**, 8425 (2004); O. A. Vydrov *et al.*, *ibid.* **125**, 074106 (2006); Y. Zhao and D. G. Truhlar, J. Phys. Chem. A **110**, 13126 (2006); M. A. Rohrdanz, K. M. Martins, and J. M. Herbert, J. Chem. Phys. **130**, 054112 (2009); Q. Wu and T. van Voorhis, J. Chem. Theory Comput. **2**, 765 (2006); J. Autschbach, Chem. Phys. Chem. **10**, 1757 (2009).

[8] T. Stein, L. Kronik, and R. Baer, J. Am. Chem. Soc. **131**, 2818 (2009).

[9] A. Hesselmann, A. Ipatov, and A. Görling, Phys. Rev. A **80**, 012507 (2009).

[10] P. Mori-Sanchez, A. J. Cohen, and W. Yang, Phys. Rev. Lett. **102**, 066403 (2009).

[11] O. Gunnarson and B. I. Lundquist, Phys. Rev. B **13**, 4274 (1976); J. P. Perdew, A. Savin, and K. Burke, Phys. Rev. A **51**, 4531 (1995).

[12] D. G. Tempel, T. J. Martinez, and N. T. Maitra, J. Chem. Theory Comput. **5**, 770 (2009).

[13] [http://www.tddft.org/programs/octopus]; M. A. L. Marques, A. Castro, G. F. Bertsch, and A. Rubio, Comput. Phys. Commun. **151**, 60 (2003).

[14] M. Casula, S. Sorella, and G. Senatore, Phys. Rev. B **74**, 245427 (2006).

[15] M. E. Casida *et al.*, J. Chem. Phys. **113**, 7062 (2000).

[16] J. B. Krieger, Y. Li, and G. J. Iafrate, Phys. Rev. A **46**, 5453 (1992).

[17] T. Körzdörfer, M. Mundt, and S. Kümmel, Phys. Rev. Lett. **100**, 133004 (2008).

[18] T. Koopmans, Physica **1**, 104 (1993); O. V. Gritsenko and E. J. Baerends, J. Chem. Phys. **117**, 9154 (2002).

[19] T. Grabo, T. Kreibich, S. Kurth, and E. K. U. Gross, in *Strong Coulomb Correlations in Electronic Structure Calculations: Beyond the Local Density Approximation*, edited by V. I. Anisimov (Gordon and Breach, Amsterdam, 2000).

[20] D. Lee, F. Furche, and K. Burke, J. Phys. Chem. Lett. **1**, 2124 (2010).

[21] M. Aymar, J. Deiglmayer, and O. Dulieu, Can. J. Phys. **87**, 543 (2009).